PHYSICAL REVIEW A VOLUME 35, NUMBER 3 FEBRUARY 1, 1987

Origin of sidebranching in dendritic growth

Olivier Martin and Nigel Goldenfeld
Loomis Laboratory of Physics, University of Illinois at Urbana-Champaign, 1110 West Green Street, Urbana, Illinois 61801
and Materials Research Laboratory, University of Illinois at Urbana-Champaign, 104 South Goodwin Avenue, Urbana, Illinois 61801
(Received 24 July 1986)

We present mechanisms for sidebranch generation in dendritic growth, stressing the importance of nonlinear effects. One such mechanism, which we call solvability-induced sidebranching, relies on the fact that the steady states form a discrete family. In addition, time-dependent simulations of crystal growth in the boundary-layer model are performed. We find that there is a critical value of the anisotropy strength below which the needle crystals are linearly unstable to tip splitting; above this value, the needle crystals have a finite-amplitude instability.

I. INTRODUCTION

The mechanisms responsible for pattern formation during diffusion-limited interface motion are beginning to be understood, through a combination of analytical, numerical, and experimental work.[1,2] Simplified models of solidification in two dimensions have permitted the identification of the physical features necessary for dendritic growth, and provide a convenient testing ground for theoretical ideas. The crucial step which has led to the present theories of dendritic growth is the realization of the central importance of anisotropy.[3,4] Early dynamical simulations of the boundary-layer model (BLM), and later the geometrical model (GM), showed that dendritic growth did not occur in the traditional formulation of solidification which neglected anisotropy. For sufficiently large anisotropy, dendritelike structures were generated. In the GM, these were accompanied by tip oscillations, whose amplitude, as a function of time, served as an indicator of the stability of these dynamical states.[4] In the boundary-layer model, no such oscillations were observed, and it was not possible to conclude whether or not the dendritelike structures were genuine dynamical steady states. The conclusions concerning the role of anisotropy have been shown not to be artifacts of the simplicity of the BLM and GM, through numerical simulation of a nonlocal model with anisotropy,[5] and by experimentation using a hydrodynamic analogue of solidification.[6]

Another important development has been the discovery, in the GM and BLM, that the continuous family of steady states which exists in the absence of surface tension is destroyed when surface tension is nonzero.[7,8] This has prompted numerical[9,10] and analytical[11] attempts to investigate whether or not this occurs also in more realistic nonlocal models of solidification. Numerical work indicates that there are only a discrete set of steady states for both two-dimensional and axisymmetric three-dimensional needle crystals. In the regime of small growth velocity, singular perturbation theory techniques have shown why there are only discrete steady states, and furthermore have predicted scaling laws for the tip velocity.[12] In the case of the related problem of the Saffman-Taylor finger, these techniques have yielded the form for the finger width as the surface tension approaches zero.[13–15]

The fastest of the surviving discrete set of steady-state solutions, known as needle crystals, seems to possess a special dynamical significance. Time-dependent simulations of both the GM and the BLM have shown that this needle crystal is an attractor for a wide range of initial conditions, for large enough anisotropy.[7,8] The dendritelike solutions, discussed further in the following paragraph, are characterized by an apparently stable tip, followed by a time-dependent train of sidebranches. This stable tip coincides with the tip of the fastest needle crystal. It is reasonable that the fastest of the needle crystals is the most stable; what is surprising is that the dendritelike structures seen in the time-dependent simulations are essentially an oscillation about this needle crystal. In the GM, it has been possible to perform a direct linear stability analysis about the fastest needle crystal. This calculation has revealed that the most unstable eigenmode—the mode with the largest real part, Ω—is controlled by the anisotropy stength. This mode is, in fact, a complex conjugate pair of eigenmodes; for $\Omega > 0$ the needle crystal is linearly unstable, and from the dynamical simulations, appears to evolve by tip splitting. For the regime $\Omega < 0$, the needle crystal is linearly stable. Sidebranches are not generated periodically at a constant distance from the tip, and true dendritic growth does not seem to occur. This corroborates the observation, from the dynamical simulations, of a decrease in the amplitude of the tip oscillations in this regime. In the BLM, however, it has not been possible, so far, to perform the analogous calculation, owing to the significantly greater complexity of the equations.

The purpose of this paper is twofold. Firstly, we consider the implications for dendritic growth of the behavior just described for the GM. If the experimentally observed dendritic growth is not a transient phenomena, then the generation of sidebranches must occur through a different mechanism than in the GM. We discuss a number of possible alternatives, paying special attention to the role of nonlinear effects. One such scenario relies on the discreteness of the steady states—a most attractive feature to us. Secondly, we present numerical studies on the BLM to try to address the same questions which have been understood satisfactorily for the GM. The BLM is one step closer to realistic physics, in that it incorporates memory effects. The description of the GM and BLM as "local" usually refers to both space and time dynamics. In fact, this

nomenclature is somewhat misleading in the case of the BLM: the points along the interface in the BLM are coupled by a diffusion field. Thus the motion of the interface in the BLM at a given time depends not only on the instantaneous configuration of the interface, but on the configuration at all earlier times. It is not inconceivable that the BLM has a dynamics closer than the GM to that of the fully nonlocal equations, which have not so far been solved. At the beginning of this investigation, we hoped that the BLM would generate sidebranches in accordance with one of our scenarios. We find, however, that the BLM does not seem to show steady-state sidebranching, but does have realistic tip splitting.

One possible approach to the question of sidebranching and instabilities is to diagonalize the stability operator, as has been done for the GM.[8] In this paper, we have chosen instead to perform detailed dynamical simulations allowing the investigation of nonlinear effects which we believe play an important role in the generation of sidebranching. The linear stability analysis will be presented elsewhere.

The content of this paper is as follows. In Sec. II, we summarize the ideas of velocity selection, and present numerical results for the dependence of the selected velocity on undercooling and anisotropy strength for the BLM. Here, and in Sec. IV, the anisotropy is included via the kinetic modification to the Gibbs-Thomson boundary condition. Section III contains our discussion of possible mechanisms for dynamical generation of sidebranches in a general setting, i.e., nothing is specific to the BLM or GM. Section IV is a presentation of our numerical results for the BLM. In our conclusions, we stress the importance of doing more experiments to test the various sidebranching mechanisms.

II. VELOCITY SELECTION IN THE BLM

In this section, we limit ourselves to the BLM, and discuss how the selected velocity v^* depends on the anisotropy strength, α, and the dimensionless undercooling, Δ. Throughout, we use the dimensionless form of BLM in two dimensions, with anisotropy included in the kinetic term modifying the Gibbs-Thomson boundary condition. The kinetic term is the lowest-order correction which arises if one wishes to take into account the nonequilibrium nature of the interfacial dynamics. The BLM is specified by the equations for the heat content density of the boundary layer, $h(s,t)$, where s is the arclength along the interface, and t is time, as well as an equation of continuity which involves the normal velocity of the interface, v_n, and w, the temperature of the interface divided by Δ. These equations are, respectively,[3]

$$\left.\frac{\partial h}{\partial t}\right|_n = v_n(1-\Delta w-\kappa h)+\frac{1}{\Delta^2}\frac{\partial}{\partial s}\left[\frac{h}{w}\frac{\partial w}{\partial s}\right], \tag{2.1}$$

$$v_n=\frac{w^2}{h}, \tag{2.2}$$

$$w=1-\Delta^2\kappa-\beta(\theta)v_n . \tag{2.3}$$

Here κ is the curvature of the interface. In Eq. (2.3), the modified Gibbs-Thomson boundary condition, we take the kinetic coefficient β to be

$$\beta(\theta)=\alpha\Delta^4[1-\cos(4\theta)], \tag{2.4}$$

where θ is the angle between the normal to the interface and the direction of propagation of the dendrite. We consider only the case of fourfold anisotropy. In these equations, the subscript n on the time derivatives indicates that the derivatives are co-moving with an identified point on the interface. As the evolution proceeds, the arclength position of this point, and the curvature there evolve according to the exact kinematical equations

$$\left.\frac{\partial\kappa}{\partial t}\right|_n = -\left[\kappa^2+\frac{\partial^2}{\partial s^2}\right]v_n , \tag{2.5}$$

$$\frac{ds}{dt}=\int_0^s \kappa v_n\, ds' . \tag{2.6}$$

Equations (2.1) to (2.6), together with initial and boundary conditions, completely specify the BLM. The quantities in these equations are related to the physical quantities by a scaling of length and time, whose significance is largely cosmetic, namely

$$s=\frac{\Delta^3 S}{d_0}, \quad t=\frac{\Delta^8 DT}{d_0^2}, \tag{2.7}$$

where S and T are the physical arclength and time, respectively, d_0 is the capillary length, and D is the thermal diffusion coefficient in the liquid.

The BLM possesses a set of steady-state solutions—needle crystals—for given Δ and α. These are conveniently obtained from the BLM equations in the stationary frame of the needle crystal with velocity v, by integrating the corresponding set of first-order ordinary differential equations in the arclength s. As has been explained in previous work,[7] the integration proceeds from a fixed point of this system of equations until the tip, $\theta=0$, is attained. Physically acceptable solutions must be differentiable there, implying that the mismatch function $M(\Delta,\alpha,v)\equiv dw/ds\,|_{s=0}$ vanishes. The possible steady-state velocities then satisfy the condition

$$M(\Delta,\alpha,v^*)=0 , \tag{2.8}$$

an equation which is equivalent to a solvability condition.

As a prelude to our studies of the dynamics of the BLM in the vicinity of the steady-state solutions (Sec. IV), we have numerically generated needle crystal solutions for a range of α with $0.75\le\Delta\le 0.95$. We are able to compute the selected velocity to an accuracy corresponding to a value for the mismatch function of about 10^{-16}. Figure 1 shows a graph of v^* against α for varying values of Δ. We observe approximately linear behavior for some nonzero interval, before the curves bend over at large α. Another feature is the behavior at very small α. Analytical calculations[12] on the BLM with kinetic anisotropy, in the limit $\Delta\to 0$, suggest that v^* behaves as a power law in α. This regime is not seen in the figure, where $\alpha\ge 0.01$. So far, we have not been able to perform numerically reliable calculations at values of α smaller than those exhibited. There is a perceptible change in behavior, possibly

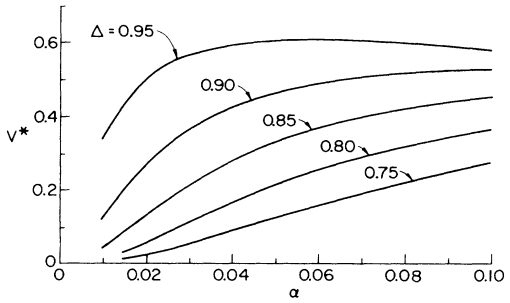

FIG. 1. Selected velocity, v^*, as function of α, for various Δ.

signaling a power-law dependence. As we shall see, the small α regime is probably not accessible to experiment because the corresponding needle crystals are very unstable.

III. SCENARIOS FOR DYNAMICAL GENERATION OF SIDEBRANCHES

We turn now to the central topic of this paper, the question of how sidebranching can arise in dendritic growth. First, we consider the linear stability of the needle crystal solution, and then show how sidebranching can arise naturally if one includes nonlinear effects. None of this section is specific to the GM or BLM.

There are two central points which we wish to address, namely, why are dendrites almost always observed to be the only alternative to tip-splitting behavior, and what controls the dynamics of the sidebranches. Recent experimental results suggest to us that there is not necessarily a unique answer to these questions. For example, in experiments on the hydrodynamic analogue for solidification,[6] needle crystals are sometimes observed, although it is hard to exclude the existence of small amplitude sidebranches which rapidly anneal. In experiments on helium crystals,[16] one also seems to have needle crystals. To our knowledge however, needle crystals have not been seen in the more conventional metallurgical systems.[17] Furthermore, the origin of sidebranching may differ from system to system. Consider the recent experimental results of Dougherty, Kaplan, and Gollub[18] on NH_4Br crystals growing from a water solution. From measurements of the dendrite width as a function of time at a given distance from the tip, they conclude that the sidebranches along different crystallographic orientations are uncorrelated. This observation suggests that noise effects are important, although it leaves open the question of whether the noise is due to microscopic fluctuations or to chaotic dynamics.

On the other hand, recent experiments by Couder *et al.*[19,20] demonstrate that a small bubble, placed at the tip of a finger in a Saffman-Taylor or Hele-Shaw cell, can induce persistent sidebranching. Their pictures exhibit essentially perfect correlation between the sidebranches on either side of the finger. This would suggest that noise effects are not important here. This is surprising since the system is effectively two dimensional, and one would expect there to be less correlation than in the three-dimensional experiments. Pieters and Langer[21] have suggested that the needle crystal solutions are linearly stable, and that sidebranching is due to selective amplification of noise in the system. The amplitude of the sidebranches could then be experimentally controlled by changing the amount of noise in the system. Whether or not this is the case should be determined as soon as possible. Certainly this is a possible explanation of sidebranching in some systems, but the experimental results mentioned above, together with the results of numerical simulations on the GM, suggest to us that deterministic mechanisms for sidebranching must also be considered. We restrict ourselves to two of the simplest such mechanisms below. Within such a framework, it is natural to think of the needle crystal as being a fixed point (in the moving frame) of the solidification equations, while the dendrite corresponds to a limit cycle. As some parameter such as the anisotropy is varied, the fixed point bifurcates[22] to a limit cycle via a linear or finite amplitude instability. The hope then is that by a local analysis about the steady-state solution near the onset, one can understand the appearance of sidebranches, calculate their amplitude, etc.

As a preliminary, we remark that it is very clear, after the fact, that dendritic growth is intimately related to anisotropy. Intuitively, in the absence of anisotropy, one would expect that the instabilities of an interface would not single out a particular direction in which to grow coherently. Only if there is sufficient anisotropy might one expect stable growth in a preferred direction. The results of detailed analysis support this general picture, as we shall see below. We shall defer discussion of the observations of Couder *et al.* until the end of this section. The next two paragraphs discuss the linear stability of needle crystals. Following that, nonlinearities are included. This gives rise in a very natural way to two scenarios for sidebranching, each depending on the nature of the most unstable eigenmode.

A. Stabilization by convection

There are two approaches to the question of stability within linear theory. The first is to consider the time evolution of a disturbance, and calculate its long-time behavior by an asymptotic analysis. The second is to find the spectrum of the linear stability operator. Neither of these approaches has been thoroughly carried out for a nonlocal model of solidification. First, we describe a poor man's version of the time evolution method, and in Sec. III B, we discuss the spectrum directly.

Consider a small perturbation near the tip of a dendrite whose extent is much smaller than the radius of curvature of the tip. The initial behavior of the perturbation is to grow, even if the needle crystal is stable. In addition, the growth is accompanied by convection effects:[23,24] the disturbance is pushed down the interface towards the tail of the dendrite. Thus, even if the amplitude grows, the dendrite can be stable in the frame moving with the tip. In the case of Saffman-Taylor fingers,[25,26] directional solidification,[27] and flame propagation,[28] this argument has been used to discuss the linear stability of the selected shape. However, a number of assumptions are made which seem to us to be questionable, particularly in the case of interest here. Let us rehearse the argument in more detail for the case of the free dendrite. Consider a

needle crystal with tip radius ρ^*, moving at the selected velocity v^*, and let a perturbation near the tip be represented as a wave packet whose mean wave number is q, and whose spread is Δq. We assume that $2\pi/q \ll \rho^*$. Let $\omega(v,q,\theta)$ be the growth rate of a perturbation of wave number q on a flat interface inclined at an angle θ to the crystal axis, and moving normal to itself with an instantaneous velocity v. Of course, this is not really the result of a linear stability analysis, because a flat interface does not have a steady state, except at $\Delta=1$. However, for perturbations growing as $\exp(\omega t)$, $\omega \neq 0$, the analysis is a good approximation because the displacement of a planar interface is proportional to $\sqrt{t}$. How does the perturbation evolve in time? If the velocity of the perturbation tangential to the interface is $v^* \sin\theta(s)$, then the usual argument says that the amplitude at an arclength position s_f, given an initial position of s_i is

$$A(s_f)=A(s_i)\exp\left[\int_0^t \omega(v^*\sin\theta(t),q(t),\theta(t))dt\right]. \quad (3.1)$$

Here the time dependence of the variables is displayed explicitly; it arises from the simultaneous translation and stretching of the wave packet. Now use the known behavior of w. Near the tip, $w>0$, and the perturbation grows. Simultaneously, it is pushed down the tail so that eventually the normal velocity of the interface at the perturbation is small enough for w to change sign. Since we can choose $A(s_i)$ to be arbitrarily small, it is always possible to arrange that $A(s_f)$ be within the linear regime. Thus, it is concluded that the needle crystal is linearly stable, at least for large q.

The argument just given is not strictly correct. Firstly, it is not true that the perturbation moves along the arclength with velocity $v^*\sin\theta$. In fact, many wavelengths contribute to the wave packet, and their motion will not be simple, especially in the vicinity of the tip. Away from the tip, the wave packet will move at the group velocity, with dispersion contributing to its spread. In addition, ω is not purely real when anisotropy is included in the calculation. It picks up an imaginary part, corresponding to a traveling wave contribution. Secondly, the argument is not specific to which needle crystal we are talking about. In the Saffman-Taylor problem, for example, there are infinitely many fingers slower than the selected one. A naive application of the arguement predicts these to be stable as well. Thirdly, the spreading of the perturbation has not been taken into account. By this we do not just mean that the wavelength is changed, but that in real space the wave packet spreads. If spreading is sufficiently important, the conclusions of the analysis should be reversed. Finally, the argument, as we have presented it, cannot be straightforwardly applied to solidification, because the motion of the perturbation is not just specified by the shape of the perturbation. The configuration of the thermal field has to be specified too. This is another way of seeing that it is not adequate to assume that the perturbation is simply convected. We conclude that we do not learn much from the naive application of this argument for the case of dendrites, especially since one is restricted to q large.

B. Eigenmodes in linear stability theory

We now discuss the other approach to stability, i.e., using the eigenmodes of the linear stability operator. The spectrum of this operator is expected to consist of a continuous part and a discrete part. The most dangerous eigenvalue, $\omega_{\max}$, is that with the largest real part, Ω. In Fig. 2 we have sketched how Ω might be expected to vary with α. This figure describes mathematically our previous claim that anisotropy is necessary for the needle crystal to grow in a well-defined direction. Note that the analysis of the preceding section predicts stability against large q perturbations only, and thus simply tells us that unstable eigenmodes must be smooth on the scale of the tip radius. In Fig. 2(a), Ω decreases monotonically with increasing α, passing through $\Omega=0$ at $\alpha=\alpha_c$. When $\Omega<0$, the needle crystal is stable, and from the point of view of the tip, transients die away, moving down towards the tail. For $\Omega>0$, the needle crystal is unstable, to either tip splitting or sidebranching. Within a linear analysis, only at $\Omega=0$ can one have a limit cycle corresponding to periodic sidebranching. However, in that case, the amplitude is not determined, and one must look towards nonlinear effects. The scenario exhibited in Fig. 2(a) has been shown to occur in the GM. There Ω corresponds to a complex conjugate pair of eigenmodes. When $\Omega>0$, the simulations show that one has oscillations of increasing amplitude at the tip until finally tip splitting occurs. To our knowledge, this in not observed to be the case experimentally. In the hydrodynamic experiments of Ben-Jacob *et al.*,[6] tip splitting proceeds smoothly and without oscillation. Nevertheless, one should search for such an oc-

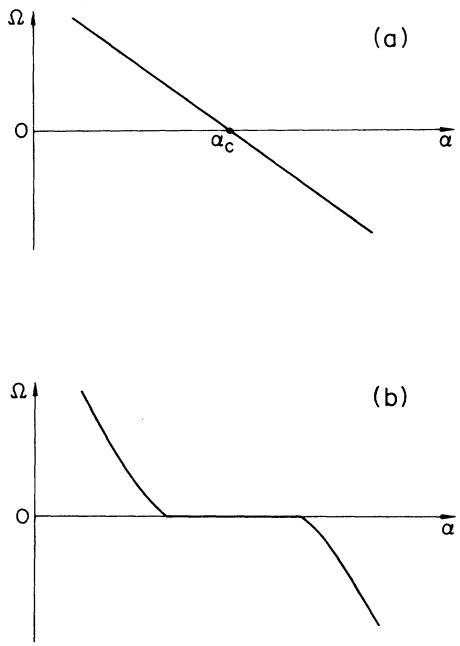

FIG. 2. Graph of Ω versus α as given by linear stability theory. (a) is the case of the GM. (b) is a hypothetical case in which sidebranching could occur generically in a linear theory.

currence experimentally. A more natural route to tip splitting is to have ω_{max} real. As we shall show in Sec. IV, this is the case in the BLM: it exhibits realistic tip splitting with ω_{max} coming from a single real eigenmode. Interestingly, sidebranches are not ruled out even if ω_{max} is real.

What does linear stability theory tell us about dendrites? Below α_c, a sidebranch instability eventually reaches the large amplitude regime where linear analysis can no longer make predictions. Thus, within linear stability theory, a limit cycle can occur only precisely at α_c. There is no reason to expect that the experiments have happened to be at or near the critical value of the anisotropy at which periodic solutions are predicted in linear theory. A possible way out of this dilemma is to conjecture that some mechanism causes Ω to be zero for an interval of α, as depicted in Fig. 2(b). We do not think that this is realistic, and in addition, the amplitude of the sidebranches are still not determined. To obtain a unique limit cycle, it is necessary to consider nonlinear effects. Depending on whether ω_{max} is complex or real, one is lead to a Hopf bifurcation scenario or a solvability-induced sidebranching scenario.

C. The Hopf bifurcation

A Hopf bifurcation[22] is the natural scenario if ω_{max} of the linear theory is complex. In this case, a limit cycle can arise via a supercritical or subcritical transition, as illustrated in Figs. 3(a) and 3(b), respectively. Consider first the supercritical case which can occur if the system is linearly unstable. If we tentatively identify α as the control parameter which takes the system through the bifurcation, then the nonlinear terms cause the amplitude of the sidebranches to stabilize at a value proportional to $\sqrt{\alpha_c-\alpha}$. One has stable and persistent sidebranches in some range below α_c, and the transition is continuous. On the other hand, if the bifurcation is subcritical, then the small amplitude branch of the limit cycle is unstable. The amplitude cannot be made arbitrarily small near the point of onset; instead, one has a finite amplitude instability. Furthermore, the onset of sidebranching will not coincide with the α_c of the linear theory, and there will be the familiar kind of hysteresis effects.

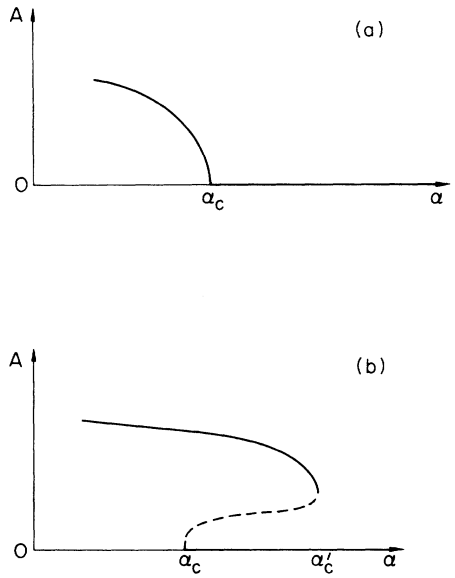

FIG. 3. Bifurcation diagrams for the Hopf bifurcation scenario. The amplitude, A, of the limit cycle is plotted against α. (a) is the case of a supercritical bifurcation. (b) is the case of a subcritical bifurcation, whose unstable branch is shown by a dashed line. α_c is the threshold predicted by linear stability analysis, α_c' is the point at which the bifurcation would be observed to occur.

In this Hopf bifurcation scenario, the sidebranch eigenmode has no reason to vanish at the tip, so that the emission of sidebranches should be accompanied by a periodic oscillation in the tip velocity and radius of curvature. In the extensive experiments of Glicksman *et al.*,[17] the dendrites apparently show no such oscillatory behavior, so we do not think that a Hopf bifurcation occurs there. Another mechanism must be responsible for the sidebranches. More recently, however, there have been reports of tip oscillations in two and three dimensional dendritic growth,[29,16] giving strong evidence that at least in certain growth regimes, one has a Hopf bifurcation. There is also an older report of such behavior.[30] In Ref. 16, needle crystals and dendrites are observed under the same conditions. If this is not due to some uncontrolled effect such as fluid motion, this is evidence that a subcritical bifurcation is present.

It is unfortunate that in the GM, the sidebranches are transients, not true limit cycles: the nonlinearities do not stabilize the sidebranch mode. Below α_c as given by the linear stability analysis, the tip oscillations grow, eventually inducing tip splitting. We suspect that by introducing further nonlinearities in the GM, one could exhibit a Hopf bifurcation. Something along these lines was attempted in Ref. 31, but it is not clear whether limit cycles were obtained. What can be expected for more realistic models of crystal growth? The competition between the sidebranches with nonlocal dynamics may provide the nonlinear stabilization required in a Hopf bifurcation. Thus we believe that this scenario is very realistic and is quite likely to occur in a variety of systems.

D. Solvability-induced sidebranching

Now we suppose that the linear stability theory is described by Fig. 2(a), with ω_{max} being real. This leads to a very interesting scenario for the generation of sidebranches for $\alpha<\alpha_c$ as follows. Let the amplitude of the eigenmode corresponding to ω_{max} be A. In the absence of any special symmetry, the Landau equation for A, neglecting mode-mode coupling, is

$$\frac{\partial A}{\partial t}=-(\alpha-\alpha_c)A-A^2\,. \tag{3.2}$$

The right-hand side is of the form $-\partial V(A)/\partial A$, with $V(A)$ sketched in Fig. 4. Let us use the convention that $A>0$ is a perturbation of positive curvature at the tip. The sign of the nonlinear term then corresponds to stabilization against too sharp a tip. Below the threshold α_c,

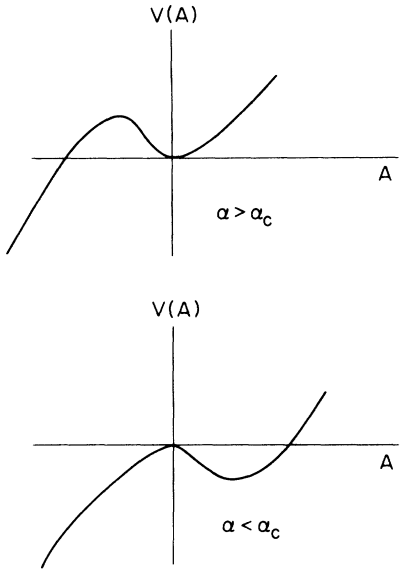

FIG. 4. Potential for the single-mode Landau equation, for $\alpha > \alpha_c$ and $\alpha < \alpha_c$.

one of two possibilities may occur. If a perturbation is such that $A < 0$, the needle crystal will tip split. This does not occur via oscillatory motion, and presumably corresponds to what is seen in the hydrodynamic experiments and in the BLM. If $A > 0$, the needle crystal evolves towards a sharper tip, and is then stabilized by the nonlinear term. However, because of the singular effects of surface tension, there are only a discrete set of needle crystals, implying that the nonzero value of A cannot correspond to a global steady state. Thus, if the tip is stable, some portion of the interface away from the tip must exhibit periodic or chaotic motion. The nonzero value of A will excite other modes, and the resultant dynamics of the tip and sidebranches will depend sensitively on the mode-mode coupling of the system in question. Thus to determine whether the tip curvature really does stabilize at a different value from the selected one, one must include the mode-mode couplings dropped in Eq. (3.2). Nevertheless, this scenario is appealing to us because it not only incorporates the linear and nonlinear stability analysis, but it also relies on the discrete nature of the steady states.

Experimentally, this scenario is characterized by a nonoscillating tip, and probably a regular emission of sidebranches. To distinguish it from a noise-induced scenario, it is necessary to control the noise in the system and see for instance that the sidebranches are symmetric about the tip. Finally, one should find a finite amplitude instability to tip splitting as predicted in Fig. 4(b). We have not found evidence for this method of generating sidebranches in the BLM, but we hope that it will explain some experimental cases of dendritic growth.

E. Limit cycles in Hele-Shaw flow

We now turn to the observations of Couder *et al.* These experiments are important as they are examples of a deterministic limit cycle giving rise to dendritic growth with nonlocal dynamics. Couder *et al.* have studied Hele-Shaw flow in both the radial and Saffman-Taylor geometry. They found that by placing an air bubble at the tip of a finger, they could generate needle crystals and dendrites. There is no manifest anisotropy in the radial cell experiments, and yet the dendrites maintain a fixed direction of propagation. We suspect that the trajectories would wander if the system was noisy. In addition, the dendrites they obtain have sidebranches which are undecorated, and do not evolve into dendrites themselves, contrary to what occurs in metallurgical cases. The regularity and strong correlations present in the sidebranching indicate a deterministic origin whose nature can be qualitatively understood from the fact that the bubble remains near the tip. Naively, one would expect the bubble to be transported away from the tip as discussed in Sec. III A. This does occur for bubbles too small or too large, but for bubble sizes a few times the plate separation, the bubble sticks to the tip of the finger and remains there. The effective curvature of the finger tip is thereby increased and this gives rise to a faster moving front. In the channel geometry, for small velocities, the overall system finger plus bubble is stable, and one sees steady-state fingers with widths smaller than $\frac{1}{2}$. At higher velocities, instabilities set in which destroy the local stability of the bubble at the tip. However, there is a nonlinear stabilization mechanism which keeps the bubble in the neighborhood of the tip as follows. When the steady-state system becomes unstable, the bubble moves away, either parallel or perpendicular to the finger direction. This displacement creates a perturbation at the finger interface, which grows and effectively forces the bubble to come back. The interface disturbance then gets advected down towards the tail, while the bubble now moves in the opposite direction. This is again stabilized, thus the system goes into a limit cycle. The above mechanism can be observed very clearly when the bubble motion is perpendicular to the growth direction, where the resulting "sidebranches" are highly asymmetric and the finger tip essentially follows the bubble, thus appearing to wiggle.

To conclude, the Couder *et al.* experiments are evidence for a deterministic generation of sidebranching, with nonlinear effects playing a crucial role. We hope that with a detailed analysis, the mechanism can be understood mathematically.

IV. NUMERICAL RESULTS IN THE BLM

In this section we present results of time-dependent simulations of the two-dimensional BLM as a test of the above scenarios. In all the runs that we report on, $\Delta = 0.75$, and reflection symmetry about the tip has been imposed. First, we discuss the stability of the needle crystals to small perturbations, illustrating the behavior of long-lived transients. We then exhibit the most dangerous eigenmode, which in the BLM is a tip-splitting mode with $\omega_{\max}$ being real. We find that $\alpha_c \simeq 0.038 \pm 0.002$. Finally, we present data showing that the nonlinear effects fit into the framework of the discussion of Sec. III. We demonstrate the existence of a nonlinear instability. However,

we do not find evidence for sidebranching, indicating that the mode-mode coupling destroys the solvability-induced scenario in the BLM.

Figure 5 shows the evolution of a perturbation about the needle crystal at $\alpha=0.1$. In the figure, we have plotted the difference between the time-dependent curvature and the curvature of the steady-state needle crystal. It can be seen that after a period of initial growth, the disturbance decays away rather slowly. Note that we are well into the stable regime, with $\alpha=0.1\gg\alpha_c$, and that the amplitude of the perturbation is very small, so that the behavior should be given by the linearized theory. Another feature which can be seen from the figure is that the disturbance does indeed get convected down towards the tail.

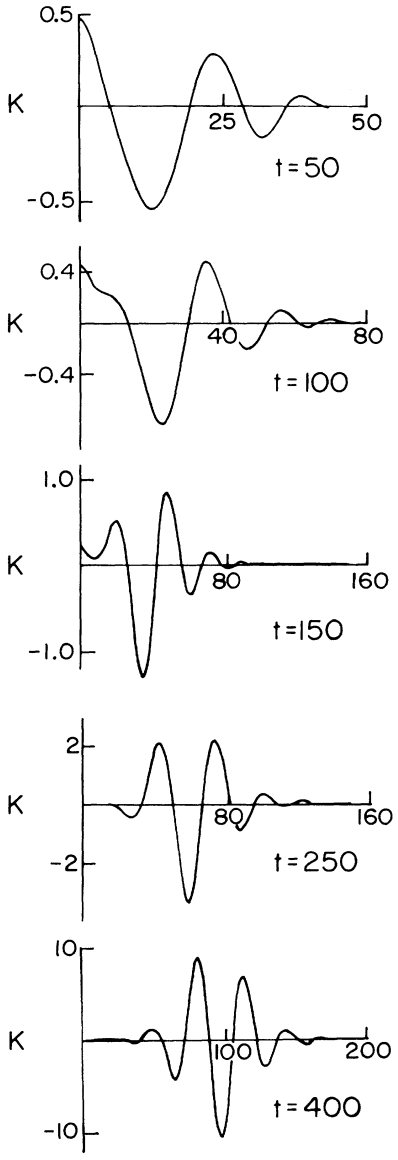

FIG. 5. Time sequence of an initial perturbation at $\Delta=0.75$ and $\alpha=0.1$. We have plotted $\Delta\kappa(s,t)=\kappa(s,t)-\kappa^*(s)$ as a function of s, where $\kappa^*(s)$ is the curvature of the needle crystal.

The slow decay of the transients hinders numerical determination of the slowest decaying eigenmode, and so we have proceeded by working below α_c and extracting the fastest growing eigenmode. Of course, one has to do some experimentation to find α_c. Our procedure is as follows.

First we start with the needle crystal solution for the chosen value of α, and evolve it dynamically. A disturbance which is smooth on the scale of the tip radius can be achieved either by adding a small amount of noise to the velocity as in Ref. 21, or by changing for a short time the value of α in the simulation. The disturbance thereafter grows with time. Its value as a function of arclength can be obtained by subtracting the steady-state needle crystal from the time-dependent profile. This is most conveniently done for the curvature rather than the actual displacement. To determine whether one is in the linear regime, we check whether the growth is exponential in time, i.e., for short times, linear in the amplitude of the disturbance. Thereafter, we rescale the disturbance as it evolves so that its curvature at the tip remains small enough for nonlinear effects to be small. The evolution then purifies the disturbance: the fastest growing eigenmode is extracted, all other modes being filtered out. For each α, one obtains a measurement of the growth rate of the eigenmode and its shape. We have found that the growth rate is real, i.e., there is no evidence for any sinusoidal time dependence.

As an example, the curvature part of the fastest growing eigenmode at $\alpha=0.035$ is shown in Fig. 6. Notice that it is localized near the tip, and that it is nonoscillatory, implying that $\omega_{\max}$ is real, in agreement with its growth behavior. Thus the linear behavior of the BLM is given by Fig. 2(a), with the instability being a tip splitting eigenmode.

What about the nonlinear effects, and does the solvability-induced sidebranching scenario occur? Figure 4 suggests that as the amplitude of the mode at the tip changes sign, there is a transition from dendritic to tip-splitting behavior. To test this, we changed the sign of the eigenmode of Fig. 6, and used it as an initial condition at $\alpha=0.035$. For short times, the mode grew, entering quickly the nonlinear regime. The time evolution then became rather chaotic, with no evidence of a limit cycle. Finally, after a very long time (10^4 time units), the curvature of the disturbance at tip changed sign, showing that in the

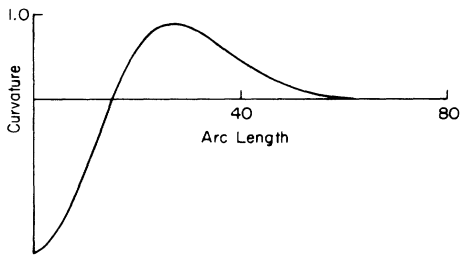

FIG. 6. The fastest growing eigenmode, for $\alpha=0.035$ and $\Delta=0.75$. We have plotted κ versus s. Units on the y axis are arbitrary.

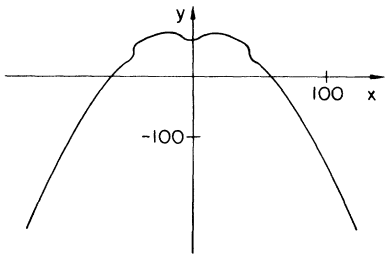

FIG. 7. The result of evolving the mode of Fig. 6 for 500 time units, plotted in real space, at $\alpha=0.06$ and $\Delta=0.75$.

BLM, the corrections to the single-mode picture destroy the nonlinear stability conjectured in Sec. III. On the other hand, Fig. 4 does predict that there is a nonlinear instability; our numerics indicate that this is not destroyed by mode-mode coupling. For example, at $\alpha=0.06$, well above α_c, a 1% reduction in the tip curvature using the mode of Fig. 6 induced tip splitting. The result after 500 time units is shown in Fig. 7. We have analyzed how the disturbance grows once it is in the nonlinear regime, and find that it is faster than exponential. This is consistent with the sign of the nonlinear term used in Eq. (3.2).

As we mentioned previously, though the BLM does not exhibit solvability-induced sidebranching, we hope that other models or certain experimental conditions will.

V. CONCLUSIONS

In this paper, we have presented a number of possible scenarios for the generation of sidebranches in dendritic growth. We have stressed that nonlinear effects play an important role, and have shown that there exists at least one scenario in which it is the combination of both the nonlinear dynamics and the singular nature of the steady states which is responsible for sidebranching. In the BLM, the most unstable eigenmode is associated with tip splitting without oscillation, in contrast to the case of the GM. We have also found a nonlinear instability above α_c; however, mode-mode coupling in the BLM seems to prevent the dynamical generation of sidebranches.

A number of important points are amenable to experiment. Firstly, one should see steady-state needle crystals, not only dendrites.[17] They are predicted by every scenario for sufficiently small noise. Perhaps this can be checked in the hydrodynamic analogue, where the suppression of noise and the control of anisotropy strength are, in principle, possible. Another possibility is to perform experiments on ^{3}He near the roughening transition, as has been done by Rolley, Balibar, and Gallet.[16] In this system, it is possible to control the anisotropy independently from the diffusion of impurities, and indeed, they seem to obtain needle crystals. Secondly, we think that experiment is capable of distinguishing between the different scenarios. It would be very interesting to know if tip splitting can be accompanied by oscillations as dendritic growth sometimes is. Observation of such oscillations would be further evidence for a Hopf bifurcation scenario. The questions of whether the transition to sidebranching occurs continuously or discontinuously, and whether or not there is hysteresis would discriminate between the subcritical and supercritical bifurcations. Finally, other scenarios will probably emerge from more experiments.

In directional solidfication, experimentation near the cusp→dendrite transition might be capable of answering the questions posed in the preceding paragraph. After most of the work reported in this paper had been completed, we learned of recent experiments by Bechhoefer and Libchaber.[32] First, they generated steady state cusps with a well defined wavelength at a drawing velocity v_0. Then, they changed the drawing velocity to v_1. If this is done slowly, the wavelength of the pattern cannot change. This gives rise to a continuous transition to dendritic growth which is interpreted as being due to the inaccessibility of the steady state for v_1. This is related, but not identical, to the solvability-induced sidebranching scenario. In both cases, the tip is dynamically stable, and because the system is not able to attain a steady state, sidebranches are generated. This sidebranching arises because of the singular nature of the velocity selection. The steady state is not permitted, in one case because of an external constraint (it is exceedingly difficult to change the wavelength of the cusps), and in the other because it is linearly unstable. We also remark that it is unlikely that the sidebranches in their experiments are noise induced. This could be definitively tested by introducing external noise.

ACKNOWLEDGMENTS

We are most grateful to J. Bechhoefer and A. Libchaber for sharing with us experimental results prior to publication. We thank R. Pieters for assistance with the time-dependent calculations. We acknowledge helpful discussions with the above and with A. Dorsey, P. Goldbart, J. Langer, and T. Ohta. We thank the Materials Research Laboratory Center for Computation for the use of their facilities. This work was supported by National Science Foundation Grants No. NFS-DMR-83-16981-23 and No. NSF-PHY-82-01948.

[1]J. S. Langer, Rev. Mod. Phys. **52**, 1 (1980).

[2]N. D. Goldenfeld, in *Metastability and Incompletely Posed Problems* (Springer-Verlag, Berlin, in press); D. Kessler, J. Koplik, and H. Levine, in Proceedings of NATO Advanced Research Workshop, Austin, Texas (unpublished).

[3]E. Ben-Jacob, N. D. Goldenfeld, J. S. Langer, and G. Schön, Phys. Rev. Lett. **51**, 1930 (1983); Phys. Rev. A **29**, 330 (1984).

[4]D. Kessler, J. Koplik, and H. Levine, Phys. Rev. A **30**, 3161 (1984).

[5]D. Kessler, J. Koplik, and H. Levine, Phys. Rev. A **30**, 2820

(1984).
[6]E. Ben-Jacob, R. Godbey, N. D. Goldenfeld, J. Koplik, H. Levine, T. Mueller, and L. M. Sander, Phys. Rev. Lett. **55**, 1315 (1985).
[7]E. Ben-Jacob, N. D. Goldenfeld, B. G. Kotliar, and J. S. Langer, Phys. Rev. Lett. **53**, 2110 (1984).
[8]D. Kessler, J. Koplik, and H. Levine, Phys. Rev. A **31**, 1712 (1985).
[9]D. Meiron, Phys. Rev. A **33**, 2704 (1986).
[10]D. Kessler, J. Koplik, and H. Levine, Phys. Rev. A **33**, 3352 (1986).
[11]B. Caroli, C. Caroli, B. Roulet, and J. S. Langer, Phys. Rev. A **33**, 442 (1986).
[12]J. S. Langer, Phys. Rev. A **33**, 435 (1986), and unpublished.
[13]D. C. Hong, and J. S. Langer, Phys. Rev. Lett. **56**, 2023 (1986).
[14]B. Shraiman, Phys. Rev. Lett. **56**, 2028 (1986).
[15]R. Combescot, T. Dombre, V. Hakim, Y. Pomeau, and A. Pumir, Phys. Rev. Lett. **56**, 2036 (1986).
[16]E. Rolley, S. Balibar, and F. Gallet, Euro. Phys. Lett. **2**, 247 (1986).
[17]S. C. Huang and M. E. Glicksman, Acta Metall. **29**, 701 (1981); **29**, 717 (1981).
[18]J. Gollub (private communication).
[19]Y. Couder, O. Cardoso, D. Dupuy, P. Tavernier, and W. Thom, Euro. Phys. Lett. **2**, 437 (1986).
[20]Y. Couder, N. Gérard, and M. Rabaud, Phys. Rev. A **34**, 5175 (1986).
[21]R. Pieters, and J. S. Langer, Phys. Rev. Lett. **56**, 1948 (1986).
[22]J. Guckenheimer and P. Holmes, *Nonlinear Oscillations, Dynamical Systems, and Bifurcation of Vector Fields* (Springer-Verlag, New York, 1983).
[23]W. Oldfield, Mater. Sci. Eng. **11**, 211 (1973).
[24]J. S. Langer, and H. Muller-Krumbhaar, Acta Metall. **26**, 1681 (1977); **26**, 1689 (1977); **26**, 1697 (1977); **29**, 145 (1981).
[25]A. J. DeGregoria and L. W. Schwartz, J. Fluid Mech. **164**, 383 (1986).
[26]D. Bensimon, L. P. Kadanoff, S. Liang, B. I. Shraiman, and C. Tang, Rev. Mod. Phys. (to be published).
[27]S. Sarker, Phys. Lett **117A**, 137 (1986).
[28]Ya.B. Zel'dovitch, A. G. Istratov, N. I. Kidin, and V. B. Librovitch, Comb. Sci. Tech. **24**, 1 (1980).
[29]H. Honjo, S. Ohta, and Y. Sawada, Phys. Rev. Lett. **55**, 841 (1985).
[30]L. R. Morris and W. C. Winegard, J. Cryst. Growth **1**, 245 (1967).
[31]H. Honjo, Y. Sawada, M. Sano, and M. Matsushita (unpublished).
[32]J. Bechhoefer and A. Libchaber, Phys. Rev. B **35** (to be published).